Representation Learning on Spatial Networks

Zheng Zhang
Department of Computer Science
Emory University
Atlanta, GA 30322, USA
zheng.zhang@emory.edu

Liang Zhao
Department of Computer Science
Emory University
Atlanta, GA 30322, USA
liang.zhao@emory.edu

Abstract

Spatial networks are networks for which the nodes and edges are constrained by geometry and embedded in real space, which has crucial effects on their topological properties. Although tremendous success has been achieved in spatial and network representation separately in recent years, there exist very little works on the representation of spatial networks. Extracting powerful representations from spatial networks requires the development of appropriate tools to uncover the pairing of both spatial and network information in the appearance of node permutation invariant, and rotation and translation invariant. Hence it can not be modeled merely with either spatial or network models individually. To address these challenges, this paper proposes a generic framework for spatial network representation learning. Specifically, a provably information-lossless and rotation-translation invariant representation of spatial information on networks is presented. Then a higher-order spatial network convolution operation that adapts to our proposed representation is introduced. To ensure efficiency, we also propose a new approach that relied on sampling random spanning trees to reduce the time and space complexity from $O(N^3)$ to $O(N)$. We demonstrate the strength of our proposed framework through extensive experiments on both synthetic and real-world datasets. The code for the proposed model is available at https://github.com/rollingstonezz/SGMP_code.

1 Introduction

Spatial data and network data are both popular types of data in modern big data era. The study of spatial data focuses on the properties of *continuous* spatial entities under specific geometry, while analysis of network data investigates the properties of *discrete* objects and their pairwise relationship.

Spanning these two data types, spatial networks is a crucial type of data structure that nodes occupy positions in a Euclidean space, where spatial patterns and constraints may have a strong effect on their connectivity patterns [6]. Understanding the mechanism of organizing spatial networks has significant importance for a broad range of fields [29], ranging from micro-scale (e.g., molecule structure [94]), to middle-scale (e.g., biological neural network [31]), to macro-scale (e.g., mobility networks [18]). Effectively learning the representations of spatial networks is extremely challenging due to the close interactions between network and spatial topology, the incompatibility between the treatments for discrete and continuous data, and particular properties
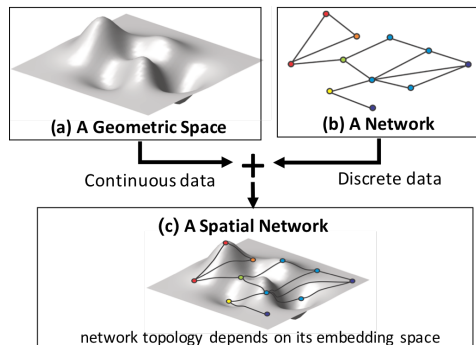
Figure 1: Spatial network contains not only the information of network topology and spatial topology but also their interaction.

35th Conference on Neural Information Processing Systems (NeurIPS 2021).

such as permutation invariant and rotation-translation invariant. Spatial networks have long been researched in the domains such as physics and mathematics, which usually extend complex networks and graph theory into spatial networks [80, 7]. They typically rely on network generation principles predefined by human heuristics and prior knowledge. Such methods usually characterize well on the aspects of the data that have been covered by the predefined principles, but not on those have not been covered[6]. However, the underlying network process in complex networks is largely unknown and extremely difficult to be predefined in simple rules, especially in crucial and open domains such as brain network modeling [81], network catastrophic failure [72], and protein folding [27].

Remarkable progress has been made towards generalizing deep representation learning approaches in spatial data and network data [96, 13, 46, 43, 28], respectively, in recent years. For spatial data, deep learning achieved significant progress in different commonly used formats such as images [53, 75, 61, 21], point clouds [34, 71, 57], meshes [85, 90], and volumetric grids [95, 66]. On the other hand, deep learning has also boosted the research of encoding graph structure on network data [46, 51, 45], and downstream applications such as recommender systems [99, 60], drug discovery [39, 22, 41, 42], FinTech [91], customer care [93], and natural language processing [62, 8, 92].

Despite the respective progress in representation learning on spatial data and network data in parallel, the representation learning for spatial networks have been largely underexplored and has just started to attract fast-increasing attention. Merely combining spatial and graph representations separately cannot handle that for spatial networks where spatial and network process are deeply coupled together [6, 68, 33]. For example, Fig. 2 shows a simple example with a pair of spatial networks, in which there are different formation rules on the edges relied on the spatial distance, that is non-distinguishable for spatial and network embedding methods, respectively.

Few recent attempts have been proposed to handle representation learning on spatial networks but still suffer from key challenges: Spatial network representation learning is a problem extremely difficult to address due to several unique challenges: 1) Difficult in distinguishing the patterns that require joint spatial and graph consideration. Examples like Figure. 2 that share the same spatial and network topology, respectively, but with significantly different interaction mechanisms, are non-distinguishable to either spatial or

Figure 2: The left figure reflects closer nodes tend to connect with each other (known as the first law of geography [79]), while the right figure reflects a spatial tele-connecting pattern where faraway nodes tend to connect. Discriminating these two spatial networks requires new method that can jointly consider spatial and network properties.

graph methods. 2) Difficult in jointly maintaining that the learned representation is invariant to node permutation, and rotation and translation transformations. Notice that spatial and graph information confine each other which neutralizes conventional methods to have either of them. For example, although point clouds representation learning can easily preserve rotation- and translation-invariant by using spatial nearest neighbors, here in spatial networks the neighbor is confined also by graph neighbors. Such additional confinement largely harden our task. 3) High efficiency and scalability in the graph size. The confinement between spatial and graph information inevitably leads to taking into account more entities simultaneously to maintain sufficient information. The requirement to handle incremental information increases the demand for model efficiency and scalability.

In order to address all the aforementioned challenges, this paper proposes a new spatial graph message passing neural network (SGMP) for learning the representations of generic spatial networks, with theoretical guarantees on discriminative power and various spatial and network properties, and an accelerating algorithm which adjusts to our theoretical framework. Specifically, to capture and model the intrinsic coupled spatial and graph properties, we propose a novel message passing neural network to organically aggregate the spatial and graph information. To ensure the invariance of learned representation under rotation and translation transformations, a novel way to represent the node spatial information by characterizing geometric invariant features with lossless information is proposed. To alleviate the efficiency issue, we propose a new accelerating algorithm for learning on graph-structured data. The proposed accelerating algorithm effectively reduces the time and memory complexity from $O(N^3)$ to $O(N)$, and maintains the theoretical guarantees for spatial networks. Finally, we demonstrate the strength of our theoretical findings through extensive experiments on both synthetic datasets and real-world datasets.

2

2 Related Work

Spatial Networks There has been a long time of research efforts on the subjects of spatial networks [6]. In the area of quantitative geography, Haggett and Chorley discussed the relevance of space in the formation and evolution of networks, and developed models to characterize spatial networks at least forty years ago [44, 17]. New insights leading to modern quantitative solutions are gained due to the advance in complex networks [32, 89, 1, 4, 3, 20], and appears in more practical fields such as transportation networks [2, 54, 55], mobility networks [18, 24], biological networks [31, 76], and computational chemistry [38, 73, 52].

Geometric Deep Learning. This is a more recent domain which handles non-Euclidean structured data such as graphs and manifolds [13].
• *Geometric Deep Learning on Manifolds.* There is a large body of research efforts of generalizing deep learning models to 3D shapes as manifolds in the computer graphics community. Many works have been conducted to find a better approach to generalize convolution-like operations to the non-Euclidean domain [65, 10, 74, 98, 64, 59]. J. Masci *et at.* proposed the framework of generalizing convolution neural network paradigm to manifolds by applying filters to extract local patches in polar coordinates [65]. Litany *et at.* [59] proposed FMNet to learn the dense correspondence between deformable 3D shapes.
• *Geometric Deep Learning on Graphs.* The earliest attempts we are aware of to generalize neural networks to graphs are attributed to M. Gori *et at.* [40]. More recently, a number of approaches encouraged by the success of convolutional neural networks [53] have attempted to generalize the notion of convolution to graphs. One important stream of convolution graph neural networks is spectral-based, where emerges after the pioneering work of Bruna *et at.* [11] which based on the spectral graph theory. There have been many following works [48, 25, 51, 56]. Another stream of work define graph convolutions as extracting locally connected regions from the graph [30, 58, 69, 45, 97, 67]. Many of these works were formulated in the family of message passing neural networks [38] which apply parametric functions to a node and its proximities, and use pooling operations to generate features for the node. Efficiency and scalability for deep graph learning is very important especially for large graphs and higher-order operations, which triggers research on accelerating GNNs [45, 16, 15]. Hamilton *et at.* [45] first introduced sampling scheme on neighborhood nodes to restrict the size. Chen *et at.* [16] proposed a method which samples vertices rather than neighbors. However, none of these works can guarantee the sampled graph is connected.

Deep Learning on Spatial Data. Deep learning has also boosted the study on spatial data. Significant progress has been achieved on deep learning on images since AlexNet [47, 75]. For 3D point clouds, PointNet [71] is a pioneering work which addressed the permutation invariance by a symmetric function. PointCNN [57] transforms the input points into a latent and potentially canonical order by a χ-conv transformations. Volumetric-based methods usually apply a 3D Convolution Neural Network (CNN) to 3D grids [95, 66]. Wang *et at.* [85] first performed shape segmentation on 3D meshes by taking three low-level geometric features as its input.

Despite the success of generalizing deep learning to network and spatial data separately, there has been relatively little work that simultaneously characterize both of them and their interaction. Previous models such as [38, 73, 52] are domain-specific, [73, 52] treat spatial networks as point clouds which ignores the influence of network structure, and [87, 86] consider POI (Point of Interest) categories, hence such concept graphs are not physically embedded in a geometric space. In addition, existing works [88, 23] typically utilize the off-the-shelf deep neural networks with Cartesian coordinates as inputs and a large amount of rotation-and translation-augmented data, which is computationally expensive and lacks theoretical guarantee of rotation- and translation-invariant on the representation. To the best of our knowledge, our proposed method is the first generic framework of spatial network representation learning that handles substantial properties of rotation- and translation-invariant and the interplay between spatial and graph patterns with a theoretical guarantee.

3 Preliminaries

In this section, we first formalize spatial networks, and the problem of representation learning on spatial networks, then we introduce the challenges in order to solve this problem.

Spatial graphs (also known as spatial networks [6]) are networks for which the nodes and edges are embedded in a geometric space. Spatial networks is ubiquitous in real world, such as molecular graphs [94], biological neural networks [31], and mobility networks [18], where the spatial and

3

network properties are usually coupled together tightly. For example, chemical bonds are derived from spatially close atoms, and fiber nerves tend to connect neurons close to each other. A spatial network is typically defined as $S = (G, P)$, where a graph $G = (V, E)$ denotes the graph topology such that V is the set of N nodes and $E \subseteq V \times V$ is the set of M edges. $e_{ij} \in E$ is an edge connecting nodes v_i and $v_j \in V$. P denotes the spatial information that is expressed as a set of points $P = \{(x_i, y_i, z_i) | x_i, y_i, z_i \in \mathbb{R}\}$ in Cartesian coordinate system, such that for a node $v_i \in V$, its coordinate is denoted as $(x_i, y_i, z_i) \in P$. Permutation invariance are crucial to graph structured data [96]. The collections of *permutation-invariant functions* on graph-structured data is defined so that $f(\pi^\dagger S \pi) = f(S)$, for all $\pi \in S_n$, where S_n is the permutation group of n elements. Rotation and translation invariance are in natural and common requirements for spatial data [36, 52]. The collections of *rotation- and translation-invariant functions* on spatial networks is defined so that $f(G, \mathcal{T}(P)) = f(G, P)$, for all $\mathcal{T} \in \mathrm{SE}(3)$, where $\mathrm{SE}(3)$ is the continuous Lie group of rotation and translation transformations in $\mathbb{R}^3$.

The main goal of this paper is to learn the representation $f(S)$ of spatial network $S = (G, P)$, with the simultaneous satisfaction of strong discriminative power and the aforementioned significant symmetry properties, which is a problem extremely difficult to address due to several unique challenges: 1) Difficult in distinguishing the patterns that require joint spatial and graph consideration. 2) Difficult in jointly maintaining that the representation is invariant to node permutations, rotation and translation transformations. 3) High efficiency and scalability according to the requirement of handling incremental information.

4 Approach

In order to achieve the novel spatial network representation learning by addressing the above-mentioned challenges, we propose a new method named spatial graph message passing neural network (SGMP) and a new accelerating algorithm which relies on sampling random spanning trees. Specifically, to discriminate spatial networks especially for the spatial-graph joint patterns, we propose a new message passing scenario which aggregates the node spatial information via higher-order edges as shown in Figure 3(a) and elaborated in Section 4.2. This scenario preserves graph and spatial information while aggregation with theoretical guarantees. To ensure that the representation is invariant to rotation and translation transformations, we propose to characterize several geometric properties in *length three path*, which is proved to represent node spatial information with guarantee on the properties of *rotation-invariant*, *translation-invariant*, and *information-lossless*. This is illustrated in Figure 3(b) and will be detailed in Section 4.1. To address the efficiency issue, an innovative sampling algorithm for accelerating training named Kirchhoff-normalized graph-sampled random spanning tree is proposed. The algorithm reduces the time and space complexity from $O(N^3)$ to $O(N)$ while still stay equivalent to original graph, which will be discussed in details in Section 4.3.

4.1 Node Spatial Information Representation

As mentioned above and in Figure 2, we need a novel way to represent the node spatial information that can preserve all the spatial structure information losslessly and also maintain rotation and translation invariance. We cannot directly use the Cartesian coordinates because they are not rotation- and translation-invariant. Although there are conventional node spatial information representation methods that maintained the rotation and translation invariance in the domain of spatial deep learning [78, 36], we cannot simply use them to handle spatial networks because they cannot consider the confinement on neighborhood from graph perspective. Otherwise, the coupled spatial-graph properties cannot be captured. Therefore, we consider to leverage *length n path* to represent the node spatial information. The most simplest way is to just use the distance among nodes and we can have $n = 4$ to ensure the spatial information is preserved. However, we want to minimize the length of the path since the size of the neighborhood grows with a factor of $O(N)$ when one more length for the path is considered. To achieve this, we successfully reduce n to 3 by proposing a new spatial information representation on path, where we use geometry features *distance*, *angle*, and *torsion* as detailed in the following equation and also illustrated in Figure 3(b).

The spatial information of a spatial network $S = (G, P)$ with N nodes can be expressed as a set of Cartesian coordinates $P = \{(x_i, y_i, z_i) | x_i, y_i, z_i \in \mathbb{R}\}_{i=1}^N$. It can also be represented as $\mathbf{P} \in \mathbb{R}^{N \times 3}$ in a matrix form. The set of all *length n path* starts from node v_i can be represented as Π_n^i. Particularly, a *length three path* $v_i \to v_j \to v_k \to v_p$ can be expressed as $\pi_{ijkp} \in \Pi_3^i$. Given a spatial network S where its graph G is strongly connected and the longest path $\zeta \geq 3$, the proposed

4
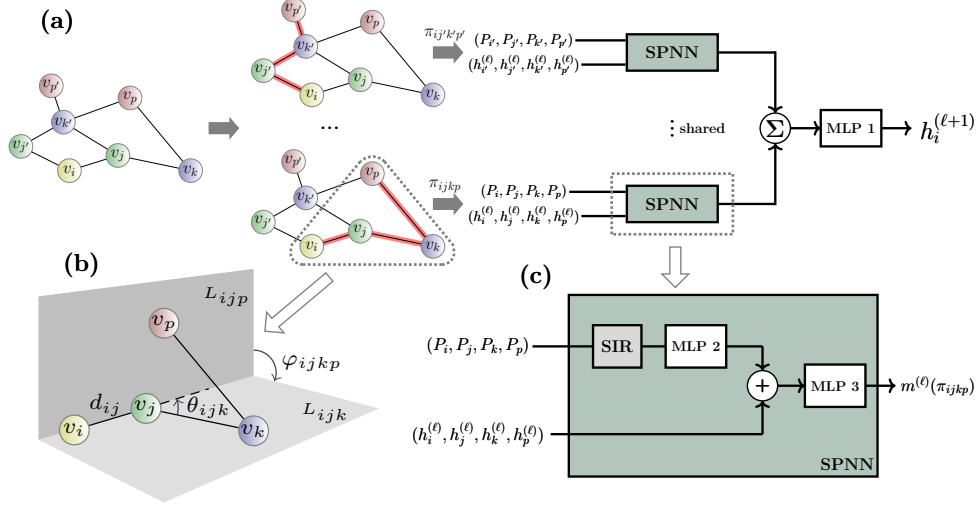
Figure 3: Illustration of the proposed spatial graph message passing neural network (SGMP). (a) The process of updating the hidden state embedding $h_i^{(\ell)}$ of node v_i by aggregating the spatial-graph message information from *length three path*. (b) An example to illustrate each elements in our spatial information representation (Equation 1). Here L_{ijp} is the plane defined by node v_i, v_j and v_p and L_{ijk} is the plane defined by node v_i, v_j and v_k. (c) This is the spatial path neural network block which is designed to learn the coupled spatial-graph property. This block also maintains the invariance to rotation and translation transformations by the spatial information representation (SIR).

spatial information representation can be expressed by one of its *length three path* $\pi_{ijkp} \in \Pi_3^i$ as

$$(d_{ij}, d_{jk}, d_{jp}, \theta_{ijk}, \theta_{ijp}, \varphi_{ijkp}), \tag{1}$$

where

$$
\begin{aligned}
& d_{ij} = ||\mathbf{P}_{ij}||_2, d_{jk} = ||\mathbf{P}_{jk}||_2, d_{jp} = ||\mathbf{P}_{jp}||_2, \\
& \theta_{ijk} = \arccos(\langle \frac{\mathbf{P}_{ij}}{d_{ij}}, \frac{\mathbf{P}_{jk}}{d_{jk}} \rangle), \theta_{ijp} = \arccos(\langle \frac{\mathbf{P}_{ij}}{d_{ij}}, \frac{\mathbf{P}_{jp}}{d_{jp}} \rangle), \\
& \varphi_{ijkp} = \text{Parity} \cdot \bar{\varphi}_{ijkp}, \\
& \mathbf{n_{ijk}} = \frac{\mathbf{P}_{ij} \times \mathbf{P}_{jk}}{||\mathbf{P}_{ij} \times \mathbf{P}_{jk}||_2}, \mathbf{n_{ijp}} = \frac{\mathbf{P}_{ij} \times \mathbf{P}_{jp}}{||\mathbf{P}_{ij} \times \mathbf{P}_{jp}||_2}, \\
& \bar{\varphi}_{ijkp} = \arccos(\langle \mathbf{n_{ijk}}, \mathbf{n_{jkp}} \rangle), \\
& \text{Parity} = \langle \frac{\mathbf{n_{ijk}} \times \mathbf{n_{ijp}}}{||\mathbf{n_{ijk}} \times \mathbf{n_{ijp}}||_2}, \frac{\mathbf{P}_{ij}}{||\mathbf{P}_{ij}||_2} \rangle.
\end{aligned}
\tag{2}
$$

Theorem 1. *Here the distances $d_{ij} \in [0, \infty)$, angles $\theta_{ijk} \in [0, \pi)$ and torsions $\varphi_{ijkp} \in [-\pi, \pi)$ are rigorously invariant under all rotation and translation transformations $\mathcal{T} \in \text{SE}(3)$.*

The proof for Theorem 1 is straightforward and can be found in Appendix B. It is remarkable to mention that the proposed representation in Equation 1 not only satisfies the invariance under rotation and translation transformation but also retains the necessary information to reconstruct the original spatial networks under weak conditions, as described in the following theorem.

Theorem 2. *Given a spatial network $S = (G, P)$, if G is a strongly connected graph with longest path $\zeta \geq 3$, then given Cartesian coordinates of three non-collinear connected nodes (v_j, v_k, v_p) in a length three path π_{ijkp} of one node v_i, the Cartesian coordinates P can be determined by the representation defined in Equation 1.*

The proof to this theorem is a consequence of the following lemma, which is proved in Appendix B.

Lemma 1. *Given Cartesian coordinates of three non-collinear connected nodes (v_j, v_k, v_p) in a length three path π_{ijkp} of one node v_i, the Cartesian coordinate P_i of node v_i can be determined by the representation defined in Equation 1.*

5

Now we can prove Theorem 2. As stated in Lemma 1, the Cartesian coordinate of node v_i can be determined by its connected neighbors v_j, v_k, v_p in the path of π_{ijkp}. Due to the property of strong connectivity of graph $G = (V, E)$, we can repeatly solve the coordinate of a connected node to the set of nodes with known coordinates. Thus, start from an arbitrary *length three path* the Cartesian coordinates P of whole spatial networks is determined.

4.2 Spatial Graph Message Passing Neural Network (SGMP)

Spatial network representation learning requires us to do convolution that aggregates jointly the graph and spatial information from the graph neighborhood. The most important issue is to maintain the discriminative power without loss of graph and spatial information during the aggregation operation. In the meanwhile, we need to maintain permutation-invariant, rotation- and translation-invariant. To achieve this, we propose the following operation to update the hidden state embedding $h_i^{(\ell)}$ of node v_i by aggregate the messages passing on all its *length three path* Π_3^i:

$$h_i^{(\ell+1)} = \sigma^{(\ell)}\Big(\text{SUM}\big(\{m^{(\ell)}(\pi_{ijkp})|\pi_{ijkp} \in \Pi_3^i\}\big)\Big), \tag{3}$$

where $\sigma^{(\ell)}$ is a multilayer perceptron (MLP) with ReLU as activation function and the spatial-graph interacted message $m^{(\ell)}(\pi_{ijkp})$ is generated by a spatial path neural network (SPNN) block:

$$\begin{aligned}
m^{(\ell)}(\pi_{ijkp}) &= \phi^{(\ell)}\Big(\bar{m}^{(\ell)}(\pi_{ijkp}), \psi^{(\ell)}\big(\hat{m}(\pi_{ijkp})\big)\Big), \\
\bar{m}^{(\ell)}(\pi_{ijkp}) &= (h_i^{(\ell)}, h_j^{(\ell)}, h_k^{(\ell)}, h_p^{(\ell)}), \\
\hat{m}(\pi_{ijkp}) &= (d_{ij}, d_{jk}, d_{jp}, \theta_{ijk}, \theta_{ijp}, \varphi_{ijkp}),
\end{aligned} \tag{4}$$

where $\phi^{(\ell)}$ and $\psi^{(\ell)}$ are two nonlinear functions to extract the complicated coupling relationship between spatial and graph information, in which we use the multilayer perceptron (MLP) with ReLU as the activation function in our settings.

Finally, the representation of spatial network S can be achieved by applying a graph aggregation operation: $f(S) = \text{AGG}(\{h_i^{(K)}|v_i \in G\})$, where AGG is a permutation invariant function such as SUM or MEAN, and K is the number of our message passing operation layers.

Since the node spatial information is already rotation- and translation-invariant, these properties can be intrinsically preserved by the operation in Equation 3. Node permutation will also be preserved due to the usage of the permutation invariant function SUM. Moreover, the following theorem proves that the discriminative power is also preserved from the perspective of maintaining the necessary spatial information, when the dimensions of hidden state embedding are sufficiently large.

Theorem 3. *Let $\mathcal{S}$ denote the collection of spatial networks with N nodes given the graph $G = (V, E)$, and $\mathcal{F}$ denote the class of our SGMP functions while γ is a continuous function. Suppose $g : \mathcal{S} \to \mathbb{R}$ is a continuous set function. For all $\epsilon > 0$, there exists a function $f \in \mathcal{F}$, such that for any $S \in \mathcal{S}$,*

$$|g(S) - \gamma(f(S))| < \epsilon. \tag{5}$$

The proof can be found in Appendix B. The key idea to the proof of this theorem is that we can discretize the continuous spatial information by partitioning the space into voxels.

4.3 Accelerate Training through Sampling Random Spanning Trees

Note that our model is a high order message passing neural network whose time and memory consumption is cubic to the average number of node degree. To reduce the complexity of graph neural networks, a typical way is based on sampling [96]. Many graph-sampling methods have been proposed for accelerating graph neural network [45, 16], which typically focus on randomly extracting a subgraph from the original graph. However, they cannot guarantee the generated graph is a strongly connected graph, which is required by our node spatial information representation in order to maintain no information loss. To ensure that the sampled graphs are connected and sparse, we innovatively propose a Kirchhoff-normalized graph-sampled random spanning tree method for accelerating the training. The proposed method largely reduces the complexity and maintains the equivalence to the original graph. Specifically, a spanning tree $T = (V, E_T)$ of an undirected graph $G = (V, E)$ that is a tree which contains all vertices in G. The number of edges of spanning trees is

6

$|E_T| = |V| - 1$, which implies that the time and space complexity during training will not be affected by the number of original edges $|E|$ in graph G. We modify our updating operation in Equation 1 as

$$h_i^{(\ell+1)} = \sigma^{(\ell)}\Big(\mathrm{SUM}\big(\{m^{(\ell)}(\pi_{ijkp})|\pi_{ijkp} \in \bar{\Pi}_{T,3}^i\}\big)\Big), \tag{6}$$

where we use $\bar{\Pi}_{T,3}^i$ denotes the set of all *length three path* starts from node v_i in a sampled spanning tree $T = (V, E_T)$. It is noticed in Equation 6 that randomly sampling spanning trees T from the original graph G will introduce an uneven probability distribution for edges, which results in non-uniform weights for path messages in our proposed message passing layer. Here we introduce the Kirchhoff-normalized method to remove the uneven distribution by pre-computing the sampling probability of a path π_{ijkp} in a sampled random spanning tree T. We further modify the Equation 6 as

$$h_i^{(\ell+1)} = \sigma^{(\ell)}\Big(\mathrm{SUM}\big(\{\frac{m^{(\ell)}(\pi_{ijkp})}{q(\pi_{ijkp})}|\pi_{ijkp} \in \bar{\Pi}_{T,3}^i\}\big)\Big), \tag{7}$$

where $q(\pi_{ijkp})$ is the sampled probability of path π_{ijkp} in a random spanning tree.

Proposition 1. *Let T denote a uniformly random spanning tree of a graph G. Then for a length three path $\pi_{ijkp} = (e_{ij}, e_{jk}, e_{kp})$ we have that*

$$\Pr(\pi_{ijkp} \in T) = det[Y_{\pi_{ijkp}}], \tag{8}$$

where Y is called the *transfer function matrix* [9]. The proof is achieved by applying graph theory theorems including Kirchhoff matrix tree theorem [14] and Burton-Pemantle theorem [12], which can be found in Appendix B. The following result establishes that the approximated form in Equation 7 is consistent to original form.

Proposition 2. *If $\sigma^{(\ell)}$ is continuous, the expectation of the approximated form in Equation 7 converges surely to the original form in Equation 3 when the number of samples is sufficiently large.*

The proof is a consequence of the strong law of large numbers and the continuous mapping theorem, which can also be found in Appendix B.

Complexity analysis of a single layer. Consider a spatial network with N nodes and dense edge data, our full SGMP layer has $O(N^3)$ time and space complexity according to the size of the neighborhood. Our accelerating algorithm based on sampling random spanning tree, however, has only $O(N)$ time and space complexity as only $N - 1$ edges exist in the generated spanning trees.

5 Experiments

In this section, the experimental settings are introduced first, then the performance of the proposed method is presented through a set of comprehensive experiments. All experiments are conducted on a 64-bit machine with an NVIDIA GPU (GTX 1080 Ti, 11016 MHz, 11 GB GDDR5). The proposed method is implemented with Pytorch deep learning framework [70].

5.1 Experiment Setup

Datasets ● *(i) Synthetic dataset.* The spatial growth graph model [6] is a spatial variant of the preferential attachment model proposed by Albert and Barabasi [1], which describes that spatial information concerns the formation of networks and long-range links are usually connecting the hubs (well-connected nodes). The process to generate such spatial networks starts from an initial connected network of m_0 nodes and introduces a new node n at each time step. The new node is allowed to make $m \leq m_0$ connections towards existing nodes with a probability $\Pi_{n \to i} \sim k_i F[d_E(n, i)]$, where k_i is the degree of node i and F is an exponential function $F(d) = e^{-d/r_c}$ of the euclidean distance $d_E(n, i)$ between the node n and the node i [5]. General characteristics of spatial networks [6] such as clustering coefficient μ, spatial diameter D, spatial radius r are set as the prediction targets. Besides, we also add the interaction range r_c, which is a significant coupled spatial-graph label that affects the formation of the spatial networks, as another prediction target. We vary the size and other parameters (according to Appendix. C for details) of spatial networks to collect $3,200$ samples in our synthetic dataset. ● *(ii) Real-world molecular property datasets.* We experiment on 5 chemical molecule benchmark datasets from [94], including both classification (BACE, BBBP) and regression (ESOL, LIPO, QM9). Particularly, QM9 is a multi-task regression benchmark with 12 quantum mechanics

7

Taret	μ	D	r	r_c
GIN	0.136(.007)	1.015(.047)	0.659(.029)	1.616(.075)
GAT	0.129(.001)	1.291(.049)	0.888(.014)	1.716(.017)
GatedGNN	0.089(.013)	0.753(.074)	0.481(.066)	1.411(.031)
PointNet	0.129(.003)	0.912(.030)	0.615(.020)	1.551(.066)
PPFNet	0.106(.006)	0.747(.037)	0.527(.014)	1.377(.057)
SGCN	0.133(.003)	1.269(.055)	0.856(.044)	1.736(.020)
SchNet	0.128(.001)	1.006(.058)	0.686(.031)	1.691(.039)
DimeNet	0.103(.027)	1.266(.147)	0.556(.094)	1.412(.059)
SGMP	**0.068(.005)**	0.748(.168)	0.450(.046)	1.332(.031)
SGMP (with st)	0.088(.001)	**0.291(.021)**	**0.252(.023)**	**1.266(.019)**

Table 1: Root mean square error (RMSE) results on synthetic dataset. Here μ is clustering coefficient, D is spatial diameter, r is spatial radius and r_c is the interaction radius in the formation of spatial growth graph.

Task	Regression			Classification	
Dataset	ESOL	LIPO	HCP	BACE	BBBP
GIN	0.776(.021)	0.699(.047)	0.792(.133)	0.792(.025)	0.864(.020)
GAT	0.783(.053)	0.757(.049)	0.561(.037)	0.780(.035)	0.854(.025)
GatedGNN	0.675(.050)	**0.630(.034)**	0.566(.036)	0.816(.023)	0.858(.020)
PointNet	0.716(.036)	0.708(.030)	0.720(.123)	0.799(.023)	0.843(.027)
PPFNet	0.731(.054)	0.720(.037)	0.680(.065)	0.805(.032)	0.869(.023)
SGCN	0.743(.056)	0.726(.055)	0.674(.059)	0.778(.030)	0.849(.021)
SchNet	0.697(.051)	0.691(.058)	0.593(.037)	0.803(.032)	0.864(.036)
DimeNet	0.730(.047)	0.666(.047)	0.818(.127)	0.791(.031)	0.864(.036)
SGMP	0.646(.049)	0.695(.027)	**0.524(.046)**	**0.830(.021)**	**0.880(.020)**
SGMP (with st)	**0.612(.054)**	0.699(.021)	0.555(.045)	0.811(.024)	0.873(.024)

Table 2: Results for four molecule property datasets and the HCP brain network. We report accuracy score for BACE and BBBP datasets, root mean square error (RMSE) for ESOL and LIPO, and mean average error (MAE) for HCP brain network dataset.

properties. The data is obtained from the pytorch-geometric library [35]. ● *(iii) Real-world HCP brain network dataset.* We also conducted an experiment using the structural connectivity (SC) of the brain network to predict the age of the subjects, which is a significant task in understanding the aging process of the human brain [50]. In specific, SC is processed from the Magnetic Resonance Imaging (MRI) data obtained from the human connectome project (HCP) [82]. By following the preprocessing procedure in [84], the SC data is constructed by applying probabilistic tracking on the diffusion MRI data using the Probtrackx tool from FMRIB Software Library [49] with 68 predefined regions of interest (ROIs). Then a threshold is applied to SC data to construct the brain networks [77, 37]. The spatial coordinates of regions are expressed as the center point of each region.

Comparison methods. To the best of our knowledge, there has been little previous work to handle the generic spatial networks. Spatial graph convolutional networks (SGCN) is a recently proposed method to handle generic spatial networks by applying a convolution operation to learn the spatial-graph interacted information using the relative coordinates between nodes and their first-order neighbors. In addition, we compare with three strong graph neural networks (GIN, GAT and Gated GNN) methods and four spatial neural networks (PointNet, PPFNet, SchNet, and DimeNet) methods for comparisons. For methods in the class of GNNs, we feed the Cartesian coordinates as node attributes while we add the node attribute and graph connectivity information to the class of SNNs for a fair comparison. The details about the benchmark models can be found in Appendix. C. Besides the models above, we also compare our model with a state-of-the-art higher-order graph neural networks PPGN [63]) in the QM9 benchmark, the results are provided from original authors.

5.2 Experimental Performance

In this section, the performance of the proposed method and its accelerated algorithm with sampling random spanning tree (with st), as well as other methods on both synthetic and real-world datasets are presented first. Then we present the efficiency test on our sampling random spanning trees method. In addition, we measure the exactness of invariance of our proposed model under translation and rotation transformations.

Effectiveness results. ● *(i) Synthetic Dataset.* Table 1 summarizes the effectiveness comparison for the synthetic dataset, where our proposed SGMP model with sampling spanning tree outperforms the best benchmark model (GatedGNN) by 35.7% on average. Especially, our model achieves lower error on the target of interaction radius (r_c), which proves that our proposed model can better capture and exploit the significant coupled spatial-graph characteristics in spatial networks. ● *(ii) Real-world Datasets.* Table 2 presents the results of four molecule property datasets and the HCP brain network dataset, where our proposed method achieves the best results in 4 out of 5 datasets. The results for the QM9 dataset are presented in Table 3, where our proposed method demonstrates its strength through outperforming the benchmark methods in 10 out of 12 targets, which is an improvement by over 14% on average. Particularly, we notice that the performance of the class of SNNs achieved significantly better results than the class of GNNs by a 38% improvement on average, which arguably implies that the quantum mechanics targets of the QM9 dataset are dominated by the spatial information. In addition, the group of jointly-spatial-graph-based methods achieved a 68.9% improvement compared to the group of point-cloud-based methods. The twelve quantum mechanical properties in the QM9 dataset seems highly related to the spatial geometry properties between nodes. For example, the formation energy (U) is related to the distances, angles, and torsions among nodes. In this situation, we notice that the performance of the group of point-cloud-based methods is significantly better than the group of GNN based methods, and jointly-spatial-graph-based methods can better explore the coupled spatial-graph property.

8

Target	GIN	GAT	Gated	PointNet	PPFNet	SGCN	PPGN	SchNet	DimeNet	SGMP	SGMP (with st)
μ	0.583	0.661	0.543	0.465	0.503	0.503	**0.093**	0.452	0.360	0.130	0.187
α	0.652	0.952	0.609	0.453	0.459	0.531	0.318	0.347	0.189	**0.113**	0.174
ϵ_{HOMO}	269.5	326.7	206.2	158.6	151.9	193.8	47.3	347.4	78.6	64.7	**45.7**
ϵ_{LOMO}	175.4	237.1	135.4	123.8	136.9	141.7	57.1	151.6	61.0	**44.7**	67.9
δ_ϵ	361.4	510.3	314.4	245.5	221.9	275.5	**78.9**	120.6	103.7	83.7	98.8
$\langle R^2 \rangle$	63.7	97.1	63.1	34.5	27.8	34.9	3.8	213.2	14.13	5.9	**3.6**
ZPVE	12.3	15.7	12.0	7.0	7.4	7.4	10.8	34.3	3.1	2.3	**2.0**
U_0	260.1	335.9	222.5	112.7	153.5	201.3	36.8	101.7	26.8	**26.1**	31.9
U	262.9	326.1	244.7	115.5	160.5	210.1	36.8	107.5	27.8	**25.2**	34.8
H	269.0	329.7	239.2	123.1	157.6	199.2	36.8	107.0	27.9	**27.5**	31.3
G	252.7	314.1	221.1	124.3	158.4	207.8	36.4	95.0	25.8	**24.6**	28.2
c_V	0.344	0.430	0.283	0.196	0.221	0.277	0.055	0.452	0.064	**0.043**	0.064

Table 3: The mean average error (MAE) results for QM9 dataset.
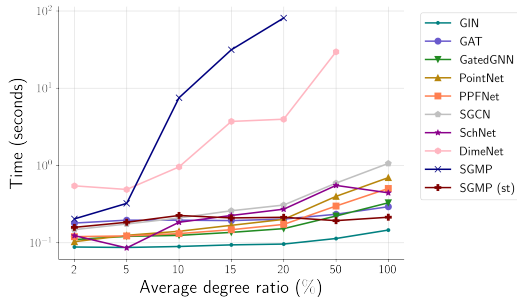
Figure 4: Efficiency analysis of our proposed models and all benchmark models. Note that our proposed algorithm with sampling random spanning tree significantly improves the scalability and efficiency.

ADR (%)	wo st	w st	speed up
2	0.203s	0.158s	1.3×
5	0.323s	0.184s	1.7×
10	7.52s	0.225s	33.4×
15	31.43s	0.209s	150.3×
20	80.96s	0.213s	379.7×
50	-	0.193s	-
100	-	0.214s	-

Table 4: Training time per epoch for our full model without sampling spanning tree (wo st) and accelerating method with sampling spanning tree (w st). (-) indicates an out-of-memory error. The sampling algorithm is on average 113 times faster than our full method. ADR is short for the average degree ratio.

Efficiency analysis. To validate the efficiency of the proposed sampling random spanning tree algorithm, we use our HCP brain network dataset with different thresholds on structural connectivity (SC) to obtain different average degrees for the nodes. The number of nodes is a fixed number (68) while we vary the average of degrees ratio (ADR= $\frac{E}{E_f}$, where E is the number of edges and E_f is the number of edges in complete graphs, e.g. ADR= 100% indicates a complete graph). We report the results of the average training time per epoch among all models for 20 epochs. As shown in Figure 4 and Table 4, our accelerating algorithm achieves significant improvements in training efficiency. Note that our method is even faster than most of the first-order methods when the graph connections are dense (ADR over 50%). Notice that higher-order methods (e.g. our full method is third-order and DimeNet is second-order) are unable to handle complete graphs due to the limits of GPU memory. The scalability of our sampling method is remarkable, which can maintain a constant time and space complexity with the increasing number of connected edges.

Rotation and translation invariant test. Similar to previous work [36], we also measure the rotation and translation robustness by uniformly adding translation and rotation transformations to the input Cartesian coordinates. Here we only report the accuracy results of classification task on the molecular dataset BACE due to the space limit while the results are similar on all datasets. According to Figure 5, we can note that the performance of our proposed model stays invariant under both translation and rotation transformations. SchNet and DimeNet can also achieve invariance under transformations because they also only use the rotation- and translation-invariant spatial features in their models. PPFNet can stay invariant under rotation transformations but not translation transformations because it preserves the origin in the model. On the other hand, SGCN can stay invariant under translation transformations but not rotation invariant because it only utilizes relative coordinates. This experiment validates the importance of applying a rotation- and translation-invariant model since we can observe that the performance of models without a theoretical guarantee drop significantly under adding rotation and translation transformations.

6 Conclusion

This paper focuses on the crucial problem of learning powerful representations from spatial networks, which has tightly coupled spatial and graph information that can not be addressed by applying spatial and network methods separately. The proposed spatial graph message passing neural network (SGMP) effectively addresses the unique challenges in spatial networks by jointly considering the spatial and graph properties, and still maintain the invariance to node permutations, as well as rotation and

9
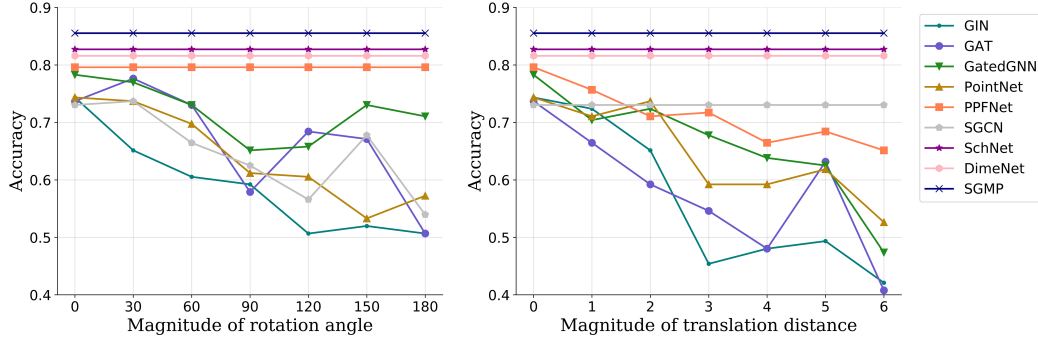
Figure 5: Robustness test of rotation and translation invariant: x-axis shows data augmentation on the test set. The x-value corresponds to the magnitude of rotation angle (left) or translation distance (right). The y-axis shows the accuracy score on the test set.

translation transformations. In addition, our proposed accelerating algorithm largely alleviates the efficiency issue in solving spatial network issues. Experimental results on synthetic and real-world datasets demonstrate the outstanding discriminative power of our model, and the efficiency test shows a remarkable improvement in training time and scalability of our proposed accelerating method.

Acknowledgement

This work was supported by the National Science Foundation (NSF) Grant No. 1755850, No. 1841520, No. 2007716, No. 2007976, No. 1942594, No. 1907805, a Jeffress Memorial Trust Award, Amazon Research Award, NVIDIA GPU Grant, and Design Knowledge Company (subcontract number: 10827.002.120.04). The authors acknowledge Emory Computer Science department for providing computational resources and technical support that have contributed to the experimental results reported within this paper.

References

[1] Réka Albert and Albert-László Barabási. Statistical mechanics of complex networks. *Reviews of modern physics*, 74(1):47, 2002.

[2] Jayanth R Banavar, Amos Maritan, and Andrea Rinaldo. Size and form in efficient transportation networks. *Nature*, 399(6732):130–132, 1999.

[3] Albert-László Barabási and Eric Bonabeau. Scale-free networks. *Scientific american*, 288(5):60–69, 2003.

[4] Alain Barrat, Marc Barthelemy, and Alessandro Vespignani. *Dynamical processes on complex networks*. Cambridge university press, 2008.

[5] Marc Barthélemy. Crossover from scale-free to spatial networks. *EPL (Europhysics Letters)*, 63(6):915, 2003.

[6] Marc Barthélemy. Spatial networks. *Physics Reports*, 499(1-3):1–101, 2011.

[7] Marc Barthelemy. *Morphogenesis of spatial networks*. Springer, 2018.

[8] Joost Bastings, Ivan Titov, Wilker Aziz, Diego Marcheggiani, and Khalil Sima'an. Graph convolutional encoders for syntax-aware neural machine translation. *arXiv preprint arXiv:1704.04675*, 2017.

[9] Stephen P Borgatti and Daniel S Halgin. On network theory. *Organization science*, 22(5):1168–1181, 2011.

[10] Davide Boscaini, Jonathan Masci, Emanuele Rodoià, and Michael Bronstein. Learning shape correspondence with anisotropic convolutional neural networks. In *Proceedings of the 30th International Conference on Neural Information Processing Systems*, pages 3197–3205, 2016.

10

[11] Joan Bruna, Wojciech Zaremba, Arthur Szlam, and Yann LeCun. Spectral networks and locally connected networks on graphs. *arXiv preprint arXiv:1312.6203*, 2013.

[12] Robert Burton and Robin Pemantle. Local characteristics, entropy and limit theorems for spanning trees and domino tilings via transfer-impedances. *The Annals of Probability*, pages 1329–1371, 1993.

[13] Wenming Cao, Zhiyue Yan, Zhiquan He, and Zhihai He. A comprehensive survey on geometric deep learning. *IEEE Access*, 8:35929–35949, 2020.

[14] Seth Chaiken and Daniel J Kleitman. Matrix tree theorems. *Journal of combinatorial theory, Series A*, 24(3):377–381, 1978.

[15] Jianfei Chen, Jun Zhu, and Le Song. Stochastic training of graph convolutional networks with variance reduction. *arXiv preprint arXiv:1710.10568*, 2017.

[16] Jie Chen, Tengfei Ma, and Cao Xiao. Fastgcn: fast learning with graph convolutional networks via importance sampling. *arXiv preprint arXiv:1801.10247*, 2018.

[17] Richard J Chorley and Petercoed Haggett. Models in geography. Technical report, 1967.

[18] Gerardo Chowell, James M Hyman, Stephen Eubank, and Carlos Castillo-Chavez. Scaling laws for the movement of people between locations in a large city. *Physical Review E*, 68(6):066102, 2003.

[19] Junyoung Chung, Caglar Gulcehre, KyungHyun Cho, and Yoshua Bengio. Empirical evaluation of gated recurrent neural networks on sequence modeling. *arXiv preprint arXiv:1412.3555*, 2014.

[20] Reuven Cohen and Shlomo Havlin. *Complex networks: structure, robustness and function*. Cambridge university press, 2010.

[21] Camille Couprie, Clément Farabet, Laurent Najman, and Yann LeCun. Indoor semantic segmentation using depth information. *arXiv preprint arXiv:1301.3572*, 2013.

[22] Hanjun Dai, Yingtao Tian, Bo Dai, Steven Skiena, and Le Song. Syntax-directed variational autoencoder for molecule generation. In *Proceedings of the International Conference on Learning Representations*, 2018.

[23] Tomasz Danel, Przemysław Spurek, Jacek Tabor, Marek Śmieja, Łukasz Struski, Agnieszka Słowik, and Łukasz Maziarka. Spatial graph convolutional networks. In *International Conference on Neural Information Processing*, pages 668–675. Springer, 2020.

[24] Andrea De Montis, Marc Barthélemy, Alessandro Chessa, and Alessandro Vespignani. The structure of interurban traffic: a weighted network analysis. *Environment and Planning B: Planning and Design*, 34(5):905–924, 2007.

[25] Michaël Defferrard, Xavier Bresson, and Pierre Vandergheynst. Convolutional neural networks on graphs with fast localized spectral filtering. *arXiv preprint arXiv:1606.09375*, 2016.

[26] Haowen Deng, Tolga Birdal, and Slobodan Ilic. Ppfnet: Global context aware local features for robust 3d point matching. In *Proceedings of the IEEE conference on computer vision and pattern recognition*, pages 195–205, 2018.

[27] Christopher M Dobson. Protein folding and misfolding. *Nature*, 426(6968):884–890, 2003.

[28] Yuanqi Du, Shiyu Wang, Xiaojie Guo, Hengning Cao, Shujie Hu, Junji Jiang, Aishwarya Varala, Abhinav Angirekula, and Liang Zhao. Graphgt: Machine learning datasets for deep graph generation and transformation. 2021.

[29] César Ducruet and Laurent Beauguitte. Spatial science and network science: review and outcomes of a complex relationship. *Networks and Spatial Economics*, 14(3):297–316, 2014.

11

[30] David Duvenaud, Dougal Maclaurin, Jorge Aguilera-Iparraguirre, Rafael Gómez-Bombarelli, Timothy Hirzel, Alán Aspuru-Guzik, and Ryan P Adams. Convolutional networks on graphs for learning molecular fingerprints. *arXiv preprint arXiv:1509.09292*, 2015.

[31] Victor M Eguiluz, Dante R Chialvo, Guillermo A Cecchi, Marwan Baliki, and A Vania Apkarian. Scale-free brain functional networks. *Physical review letters*, 94(1):018102, 2005.

[32] Paul Erdős and Alfréd Rényi. On the evolution of random graphs. *Publ. Math. Inst. Hung. Acad. Sci*, 5(1):17–60, 1960.

[33] Paul Expert, Tim S Evans, Vincent D Blondel, and Renaud Lambiotte. Uncovering space-independent communities in spatial networks. *Proceedings of the National Academy of Sciences*, 108(19):7663–7668, 2011.

[34] Haoqiang Fan, Hao Su, and Leonidas J Guibas. A point set generation network for 3d object reconstruction from a single image. In *Proceedings of the IEEE conference on computer vision and pattern recognition*, pages 605–613, 2017.

[35] Matthias Fey and Jan Eric Lenssen. Fast graph representation learning with pytorch geometric. *arXiv preprint arXiv:1903.02428*, 2019.

[36] Fabian B Fuchs, Daniel E Worrall, Volker Fischer, and Max Welling. Se (3)-transformers: 3d roto-translation equivariant attention networks. *arXiv preprint arXiv:2006.10503*, 2020.

[37] Linda Geerligs, Remco J Renken, Emi Saliasi, Natasha M Maurits, and Monicque M Lorist. A brain-wide study of age-related changes in functional connectivity. *Cerebral cortex*, 25(7):1987–1999, 2015.

[38] Justin Gilmer, Samuel S Schoenholz, Patrick F Riley, Oriol Vinyals, and George E Dahl. Neural message passing for quantum chemistry. In *International Conference on Machine Learning*, pages 1263–1272. PMLR, 2017.

[39] Rafael Gómez-Bombarelli, Jennifer N Wei, David Duvenaud, José Miguel Hernández-Lobato, Benjamín Sánchez-Lengeling, Dennis Sheberla, Jorge Aguilera-Iparraguirre, Timothy D Hirzel, Ryan P Adams, and Alán Aspuru-Guzik. Automatic chemical design using a data-driven continuous representation of molecules. *ACS central science*, 4(2):268–276, 2018.

[40] Marco Gori, Gabriele Monfardini, and Franco Scarselli. A new model for learning in graph domains. In *Proceedings. 2005 IEEE International Joint Conference on Neural Networks, 2005.*, volume 2, pages 729–734. IEEE, 2005.

[41] Xiaojie Guo, Yuanqi Du, and Liang Zhao. Property controllable variational autoencoder via invertible mutual dependence. In *International Conference on Learning Representations*, 2020.

[42] Xiaojie Guo, Yuanqi Du, and Liang Zhao. Deep generative models for spatial networks. In *Proceedings of the 27th ACM SIGKDD Conference on Knowledge Discovery & Data Mining*, pages 505–515, 2021.

[43] Yulan Guo, Hanyun Wang, Qingyong Hu, Hao Liu, Li Liu, and Mohammed Bennamoun. Deep learning for 3d point clouds: A survey. *IEEE transactions on pattern analysis and machine intelligence*, 2020.

[44] Peter Haggett and Richard J Chorley. *Network analysis in geography*, volume 1. Hodder Education, 1969.

[45] William L Hamilton, Rex Ying, and Jure Leskovec. Inductive representation learning on large graphs. *arXiv preprint arXiv:1706.02216*, 2017.

[46] William L Hamilton, Rex Ying, and Jure Leskovec. Representation learning on graphs: Methods and applications. *arXiv preprint arXiv:1709.05584*, 2017.

[47] Kaiming He, Xiangyu Zhang, Shaoqing Ren, and Jian Sun. Deep residual learning for image recognition. In *Proceedings of the IEEE conference on computer vision and pattern recognition*, pages 770–778, 2016.

12

[48] Mikael Henaff, Joan Bruna, and Yann LeCun. Deep convolutional networks on graph-structured data. *arXiv preprint arXiv:1506.05163*, 2015.

[49] Mark Jenkinson, Christian F Beckmann, Timothy EJ Behrens, Mark W Woolrich, and Stephen M Smith. Fsl. *Neuroimage*, 62(2):782–790, 2012.

[50] Benedikt Atli Jónsson, Gyda Bjornsdottir, TE Thorgeirsson, Lotta María Ellingsen, G Bragi Walters, DF Gudbjartsson, Hreinn Stefansson, Kari Stefansson, and MO Ulfarsson. Brain age prediction using deep learning uncovers associated sequence variants. *Nature communications*, 10(1):1–10, 2019.

[51] Thomas N Kipf and Max Welling. Semi-supervised classification with graph convolutional networks. *arXiv preprint arXiv:1609.02907*, 2016.

[52] Johannes Klicpera, Janek Groß, and Stephan Günnemann. Directional message passing for molecular graphs. *arXiv preprint arXiv:2003.03123*, 2020.

[53] Alex Krizhevsky, Ilya Sutskever, and Geoffrey E Hinton. Imagenet classification with deep convolutional neural networks. *Advances in neural information processing systems*, 25:1097–1105, 2012.

[54] Maciej Kurant and Patrick Thiran. Extraction and analysis of traffic and topologies of transportation networks. *Physical Review E*, 74(3):036114, 2006.

[55] Vito Latora and Massimo Marchiori. Vulnerability and protection of infrastructure networks. *Physical Review E*, 71(1):015103, 2005.

[56] Ron Levie, Federico Monti, Xavier Bresson, and Michael M Bronstein. Cayleynets: Graph convolutional neural networks with complex rational spectral filters. *IEEE Transactions on Signal Processing*, 67(1):97–109, 2018.

[57] Yangyan Li, Rui Bu, Mingchao Sun, Wei Wu, Xinhan Di, and Baoquan Chen. Pointcnn: Convolution on x-transformed points. *Advances in neural information processing systems*, 31:820–830, 2018.

[58] Yujia Li, Daniel Tarlow, Marc Brockschmidt, and Richard Zemel. Gated graph sequence neural networks. *arXiv preprint arXiv:1511.05493*, 2015.

[59] Or Litany, Tal Remez, Emanuele Rodola, Alex Bronstein, and Michael Bronstein. Deep functional maps: Structured prediction for dense shape correspondence. In *Proceedings of the IEEE international conference on computer vision*, pages 5659–5667, 2017.

[60] Ao Liu, Qiong Wu, Zhenming Liu, and Lirong Xia. Near-neighbor methods in random preference completion. In *Proceedings of the AAAI Conference on Artificial Intelligence*, 2019.

[61] Jonathan Long, Evan Shelhamer, and Trevor Darrell. Fully convolutional networks for semantic segmentation. In *Proceedings of the IEEE conference on computer vision and pattern recognition*, pages 3431–3440, 2015.

[62] Diego Marcheggiani and Ivan Titov. Encoding sentences with graph convolutional networks for semantic role labeling. *arXiv preprint arXiv:1703.04826*, 2017.

[63] Haggai Maron, Heli Ben-Hamu, Hadar Serviansky, and Yaron Lipman. Provably powerful graph networks. *arXiv preprint arXiv:1905.11136*, 2019.

[64] Haggai Maron, Meirav Galun, Noam Aigerman, Miri Trope, Nadav Dym, Ersin Yumer, Vladimir G Kim, and Yaron Lipman. Convolutional neural networks on surfaces via seamless toric covers. *ACM Trans. Graph.*, 36(4):71–1, 2017.

[65] Jonathan Masci, Davide Boscaini, Michael Bronstein, and Pierre Vandergheynst. Geodesic convolutional neural networks on riemannian manifolds. In *Proceedings of the IEEE international conference on computer vision workshops*, pages 37–45, 2015.

13

[66] Daniel Maturana and Sebastian Scherer. Voxnet: A 3d convolutional neural network for real-time object recognition. In *2015 IEEE/RSJ International Conference on Intelligent Robots and Systems (IROS)*, pages 922–928. IEEE, 2015.

[67] Christopher Morris, Martin Ritzert, Matthias Fey, William L Hamilton, Jan Eric Lenssen, Gaurav Rattan, and Martin Grohe. Weisfeiler and leman go neural: Higher-order graph neural networks. In *Proceedings of the AAAI Conference on Artificial Intelligence*, volume 33, pages 4602–4609, 2019.

[68] Richard G Morris and Marc Barthelemy. Transport on coupled spatial networks. *Physical review letters*, 109(12):128703, 2012.

[69] Mathias Niepert, Mohamed Ahmed, and Konstantin Kutzkov. Learning convolutional neural networks for graphs. In *International conference on machine learning*, pages 2014–2023. PMLR, 2016.

[70] Adam Paszke, Sam Gross, Francisco Massa, Adam Lerer, James Bradbury, Gregory Chanan, Trevor Killeen, Zeming Lin, Natalia Gimelshein, Luca Antiga, et al. Pytorch: An imperative style, high-performance deep learning library. *arXiv preprint arXiv:1912.01703*, 2019.

[71] Charles R Qi, Hao Su, Kaichun Mo, and Leonidas J Guibas. Pointnet: Deep learning on point sets for 3d classification and segmentation. In *Proceedings of the IEEE conference on computer vision and pattern recognition*, pages 652–660, 2017.

[72] Saulo DS Reis, Yanqing Hu, Andrés Babino, José S Andrade Jr, Santiago Canals, Mariano Sigman, and Hernán A Makse. Avoiding catastrophic failure in correlated networks of networks. *Nature Physics*, 10(10):762–767, 2014.

[73] Kristof T Schütt, Pieter-Jan Kindermans, Huziel E Sauceda, Stefan Chmiela, Alexandre Tkatchenko, and Klaus-Robert Müller. Schnet: A continuous-filter convolutional neural network for modeling quantum interactions. *arXiv preprint arXiv:1706.08566*, 2017.

[74] David I Shuman, Benjamin Ricaud, and Pierre Vandergheynst. Vertex-frequency analysis on graphs. *Applied and Computational Harmonic Analysis*, 40(2):260–291, 2016.

[75] Richard Socher, Brody Huval, Bharath Bath, Christopher D Manning, and Andrew Ng. Convolutional-recursive deep learning for 3d object classification. *Advances in neural information processing systems*, 25:656–664, 2012.

[76] Olaf Sporns, Giulio Tononi, and Gerald M Edelman. Theoretical neuroanatomy: relating anatomical and functional connectivity in graphs and cortical connection matrices. *Cerebral cortex*, 10(2):127–141, 2000.

[77] Kaustubh Supekar, Vinod Menon, Daniel Rubin, Mark Musen, and Michael D Greicius. Network analysis of intrinsic functional brain connectivity in alzheimer's disease. *PLoS Comput Biol*, 4(6):e1000100, 2008.

[78] Nathaniel Thomas, Tess Smidt, Steven Kearnes, Lusann Yang, Li Li, Kai Kohlhoff, and Patrick Riley. Tensor field networks: Rotation-and translation-equivariant neural networks for 3d point clouds. *arXiv preprint arXiv:1802.08219*, 2018.

[79] Waldo R Tobler. A computer movie simulating urban growth in the detroit region. *Economic geography*, 46(sup1):234–240, 1970.

[80] Dimitrios Tsiotas and Serafeim Polyzos. The complexity in the study of spatial networks: an epistemological approach. *Networks and Spatial Economics*, 18(1):1–32, 2018.

[81] Martijn P Van Den Heuvel and Hilleke E Hulshoff Pol. Exploring the brain network: a review on resting-state fmri functional connectivity. *European neuropsychopharmacology*, 20(8):519–534, 2010.

[82] David C Van Essen, Stephen M Smith, Deanna M Barch, Timothy EJ Behrens, Essa Yacoub, Kamil Ugurbil, Wu-Minn HCP Consortium, et al. The wu-minn human connectome project: an overview. *Neuroimage*, 80:62–79, 2013.

14

[83] Petar Veličković, Guillem Cucurull, Arantxa Casanova, Adriana Romero, Pietro Lio, and Yoshua Bengio. Graph attention networks. *arXiv preprint arXiv:1710.10903*, 2017.

[84] Jichuan Wang and Xiaoqian Wang. *Structural equation modeling: Applications using Mplus*. John Wiley & Sons, 2019.

[85] Nanyang Wang, Yinda Zhang, Zhuwen Li, Yanwei Fu, Wei Liu, and Yu-Gang Jiang. Pixel2mesh: Generating 3d mesh models from single rgb images. In *Proceedings of the European Conference on Computer Vision (ECCV)*, pages 52–67, 2018.

[86] Pengyang Wang, Yanjie Fu, Hui Xiong, and Xiaolin Li. Adversarial substructured representation learning for mobile user profiling. In *Proceedings of the 25th ACM SIGKDD International Conference on Knowledge Discovery & Data Mining*, pages 130–138, 2019.

[87] Pengyang Wang, Kunpeng Liu, Lu Jiang, Xiaolin Li, and Yanjie Fu. Incremental mobile user profiling: Reinforcement learning with spatial knowledge graph for modeling event streams. In *Proceedings of the 26th ACM SIGKDD International Conference on Knowledge Discovery & Data Mining*, pages 853–861, 2020.

[88] Zheng Wang, Ce Ju, Gao Cong, and Cheng Long. Representation learning for spatial graphs. *arXiv preprint arXiv:1812.06668*, 2018.

[89] Duncan J Watts and Steven H Strogatz. Collective dynamics of 'small-world'networks. *nature*, 393(6684):440–442, 1998.

[90] Chao Wen, Yinda Zhang, Zhuwen Li, and Yanwei Fu. Pixel2mesh++: Multi-view 3d mesh generation via deformation. In *Proceedings of the IEEE/CVF International Conference on Computer Vision*, pages 1042–1051, 2019.

[91] Q Wu, C Brinton, Z Zhang, M Cucuringu, A Pizzoferrato, and Z Liu. Equity2vec: End-to-end deep learning framework for cross-sectional asset pricing. In *2nd ACM International Conference on AI in Finance*, 2021.

[92] Qiong Wu, Adam Hare, Sirui Wang, Yuwei Tu, Zhenming Liu, Christopher G Brinton, and Yanhua Li. Bats: A spectral biclustering approach to single document topic modeling and segmentation. *ACM Transactions on Intelligent Systems and Technology*, 2021.

[93] Qiong Wu, Wen-Ling Hsu, Tan Xu, Zhenming Liu, George Ma, Guy Jacobson, and Shuai Zhao. Speaking with actions - learning customer journey behavior. In *2019 IEEE 13th International Conference on Semantic Computing (ICSC)*, pages 279–286, 2019.

[94] Zhenqin Wu, Bharath Ramsundar, Evan N Feinberg, Joseph Gomes, Caleb Geniesse, Aneesh S Pappu, Karl Leswing, and Vijay Pande. Moleculenet: a benchmark for molecular machine learning. *Chemical science*, 9(2):513–530, 2018.

[95] Zhirong Wu, Shuran Song, Aditya Khosla, Fisher Yu, Linguang Zhang, Xiaoou Tang, and Jianxiong Xiao. 3d shapenets: A deep representation for volumetric shapes. In *Proceedings of the IEEE conference on computer vision and pattern recognition*, pages 1912–1920, 2015.

[96] Zonghan Wu, Shirui Pan, Fengwen Chen, Guodong Long, Chengqi Zhang, and S Yu Philip. A comprehensive survey on graph neural networks. *IEEE transactions on neural networks and learning systems*, 2020.

[97] Keyulu Xu, Weihua Hu, Jure Leskovec, and Stefanie Jegelka. How powerful are graph neural networks? *arXiv preprint arXiv:1810.00826*, 2018.

[98] Li Yi, Hao Su, Xingwen Guo, and Leonidas J Guibas. Syncspeccnn: Synchronized spectral cnn for 3d shape segmentation. In *Proceedings of the IEEE Conference on Computer Vision and Pattern Recognition*, pages 2282–2290, 2017.

[99] Rex Ying, Ruining He, Kaifeng Chen, Pong Eksombatchai, William L Hamilton, and Jure Leskovec. Graph convolutional neural networks for web-scale recommender systems. In *Proceedings of the 24th ACM SIGKDD International Conference on Knowledge Discovery & Data Mining*, pages 974–983, 2018.

15

Checklist

The checklist follows the references. Please read the checklist guidelines carefully for information on how to answer these questions. For each question, change the default **[TODO]** to [Yes] , [No] , or [N/A] . You are strongly encouraged to include a **justification to your answer**, either by referencing the appropriate section of your paper or providing a brief inline description. For example:

- Did you include the license to the code and datasets? [Yes] See Section **??**.
- Did you include the license to the code and datasets? [No] The code and the data are proprietary.
- Did you include the license to the code and datasets? [N/A]

Please do not modify the questions and only use the provided macros for your answers. Note that the Checklist section does not count towards the page limit. In your paper, please delete this instructions block and only keep the Checklist section heading above along with the questions/answers below.

1. For all authors...
   (a) Do the main claims made in the abstract and introduction accurately reflect the paper's contributions and scope? [Yes]
   (b) Did you describe the limitations of your work? [Yes] See Section 4.3 for the discussion of the efficiency issue of our full SGMP model.
   (c) Did you discuss any potential negative societal impacts of your work? [N/A]
   (d) Have you read the ethics review guidelines and ensured that your paper conforms to them? [Yes] I have read the ethics review guidelines and ensure that our paper conforms to them.

2. If you are including theoretical results...
   (a) Did you state the full set of assumptions of all theoretical results? [Yes]
   (b) Did you include complete proofs of all theoretical results? [Yes]

3. If you ran experiments...
   (a) Did you include the code, data, and instructions needed to reproduce the main experimental results (either in the supplemental material or as a URL)? [Yes]
   (b) Did you specify all the training details (e.g., data splits, hyperparameters, how they were chosen)? [Yes]
   (c) Did you report error bars (e.g., with respect to the random seed after running experiments multiple times)? [Yes] We report error bars in our experimental results.
   (d) Did you include the total amount of compute and the type of resources used (e.g., type of GPUs, internal cluster, or cloud provider)? [Yes]

4. If you are using existing assets (e.g., code, data, models) or curating/releasing new assets...
   (a) If your work uses existing assets, did you cite the creators? [Yes]
   (b) Did you mention the license of the assets? [Yes]
   (c) Did you include any new assets either in the supplemental material or as a URL? [N/A]

   (d) Did you discuss whether and how consent was obtained from people whose data you're using/curating? [Yes]
   (e) Did you discuss whether the data you are using/curating contains personally identifiable information or offensive content? [N/A]

5. If you used crowdsourcing or conducted research with human subjects...
   (a) Did you include the full text of instructions given to participants and screenshots, if applicable? [N/A]
   (b) Did you describe any potential participant risks, with links to Institutional Review Board (IRB) approvals, if applicable? [N/A]
   (c) Did you include the estimated hourly wage paid to participants and the total amount spent on participant compensation? [N/A]

16

A Representation Limits

In Section 4 we discussed the strong discriminative power of our proposed method on *length three path*. In this section, we emphasize the necessity of using *length three path* from an intuitive perspective: we present two novel examples in Figure 6 and Figure 7 to show the limits on the discriminative power of methods using *length one path* and *length two path* under the constraints of rotation and translation invariance.
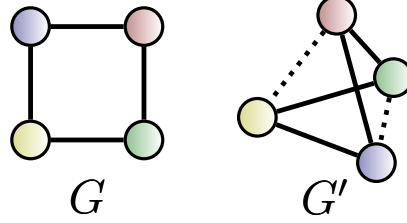
Figure 6: *length one path* models fail to discriminate between G (a regular quadrilateral) and G' (a regular tetrahedron) since the distances between all pairs of connected nodes are the same in two spatial networks. The significant spatial structure might be neglected when *length one path* model is using.
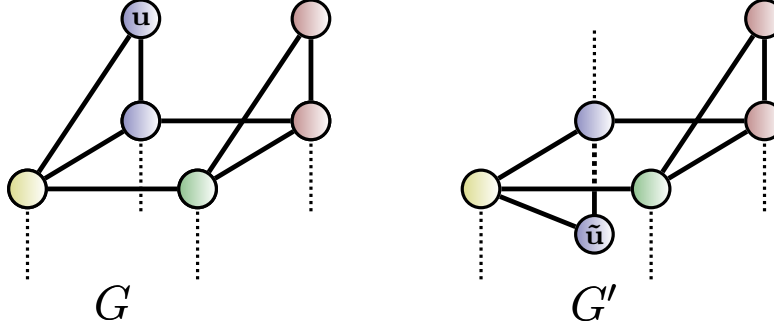
Figure 7: The spatial graph G and G' differs in the $Parity$ of node u and $\tilde{u}$, which are indistinguishable to both *length two path* and *length one path* models since the corresponding directional angles and distances are identical in the two spatial graphs. A practical example of this would be the hydrophilic and hydrophobic groups in biological networks.

B Proofs

Theorem 1.   *Here the distances $d_{ij} \in [0, \infty)$, angles $\theta_{ijk} \in [0, \pi)$ and torsions $\varphi_{ijkp} \in [-\pi, \pi)$ are rigorously invariant under all rotation and translation transformations $\mathcal{T} \in \mathrm{SE}(3)$.*
Proof of Theorem 1. It is obvious to show that distances, angles, and torsions are invariant to translation transformations since only relative coordinates are using in the formulation.

For rotation transformations $R \in SO(3)$ (the rotation group in 3D space), we show two identity equations first:

$$\langle R\mathbf{x}, R\mathbf{y} \rangle = \langle \mathbf{x}, \mathbf{y} \rangle$$
$$(R\mathbf{x}) \times (R\mathbf{y}) = R(\mathbf{x} \times \mathbf{y}) \tag{9}$$

17

Thus we have

$$d_{ij} = ||\mathbf{P}_{ij}||_2 = \langle \mathbf{P}_{ij}, \mathbf{P}_{ij} \rangle = \langle R\mathbf{P}_{ij}, R\mathbf{P}_{ij} \rangle,$$

$$\theta_{ijk} = \arccos(\langle \frac{\mathbf{P}_{ij}}{d_{ij}}, \frac{\mathbf{P}_{jk}}{d_{jk}} \rangle) = \arccos(\langle \frac{R\mathbf{P}_{ij}}{d_{ij}}, \frac{R\mathbf{P}_{jk}}{d_{jk}} \rangle),$$

$$\bar{\varphi}_{ijkp} = \arccos(\langle \mathbf{n_{ijk}}, \mathbf{n_{jkp}} \rangle) = \arccos(\langle R\mathbf{n_{ijk}}, R\mathbf{n_{jkp}} \rangle),$$

$$\text{Parity} = \langle \frac{\mathbf{n_{ijk}} \times \mathbf{n_{ijp}}}{||\mathbf{n_{ijk}} \times \mathbf{n_{ijp}}||_2}, \frac{\mathbf{P}_{ij}}{||\mathbf{P}_{ij}||_2} \rangle$$

$$= \langle \frac{R(\mathbf{n_{ijk}} \times \mathbf{n_{ijp}})}{||R(\mathbf{n_{ijk}} \times \mathbf{n_{ijp}})||_2}, \frac{R\mathbf{P}_{ij}}{||R\mathbf{P}_{ij}||_2} \rangle$$

$$= \langle \frac{(R\mathbf{n_{ijk}}) \times (R\mathbf{n_{ijp}})}{||(R\mathbf{n_{ijk}}) \times (R\mathbf{n_{ijp}})||_2}, \frac{R\mathbf{P}_{ij}}{||R\mathbf{P}_{ij}||_2} \rangle.$$

All elements are invariant under rotation and translation transformations. $\square$

Lemma 1. *Given Cartesian coordinates of three non-collinear connected nodes (v_j, v_k, v_p) in a length three path π_{ijkp} of one node v_i, the Cartesian coordinate P_i of node v_i can be determined by the representation defined in Equation 1.*

Proof of Lemma 1. Note that from Equation 2 we have

$$||\mathbf{P}_{ij} \times \mathbf{P}_{jk}||_2 = d_{ij}d_{jk}\sin\theta_{ijk},$$

$$\mathbf{n_{ijk}} \times \mathbf{n_{ijp}} = \frac{1}{d_{ij}^2 d_{jk}d_{jp}\sin\theta_{ijk}\sin\theta_{ijp}}(\mathbf{P}_{ij} \times \mathbf{P}_{jk}) \times (\mathbf{P}_{ij} \times \mathbf{P}_{jp})$$

$$= \frac{1}{d_{ij}^2 d_{jk}d_{jp}\sin\theta_{ijk}\sin\theta_{ijp}}(\mathbf{P}_{ij} \cdot (\mathbf{P}_{jk} \times \mathbf{P}_{jp}))\mathbf{P}_{ij},$$

$$\langle \mathbf{n_{ijk}}, \mathbf{n_{ijp}} \rangle = \cos\bar{\varphi}_{ijkp} = \cos\varphi_{ijkp},$$

$$\text{Parity} = \frac{\langle \mathbf{n_{ijk}} \times \mathbf{n_{ijp}}, \mathbf{P}_{ij} \rangle}{d_{ij}\sin\bar{\varphi}_{ijkp}} = \frac{\mathbf{P}_{ij} \cdot (\mathbf{P}_{jk} \times \mathbf{P}_{jp})}{d_{ij}d_{jk}d_{jp}\sin\theta_{ijk}\sin\theta_{ijp}\sin\bar{\varphi}_{ijkp}}.$$

Suppose that the solution set of the Equation 1 contains two different solutions v_i and v_i', then the Equation 2 implies that due to the same representation, we have

$$\text{Parity}(i) = \text{Parity}(i')$$

$$\frac{\mathbf{P}_{ij} \cdot (\mathbf{P}_{jk} \times \mathbf{P}_{jp})}{d_{ij}d_{jk}d_{jp}\sin\theta_{ijk}\sin\theta_{ijp}\sin\bar{\varphi}_{ijkp}} = \frac{\mathbf{P}_{i'j} \cdot (\mathbf{P}_{jk} \times \mathbf{P}_{jp})}{d_{i'j}d_{jk}d_{jp}\sin\theta_{i'jk}\sin\theta_{i'jp}\sin\bar{\varphi}_{i'jkp}}$$

$$0 = \mathbf{P}_{ii'} \cdot (\mathbf{P}_{jk} \times \mathbf{P}_{jp}).$$

Since v_j, v_k, v_p is non-colinear, $\mathbf{P}_{jk} \times \mathbf{P}_{jp}$ is nonzero, the equation causes a contradiction. Thus, the Cartesian coordinate of node v_i can be uniquely determined by the Equation 1. $\square$

Theorem 3. *Let S denote the collection of spatial networks with N nodes given the graph $G = (V, E)$, and $\mathcal{F}$ denote the class of our SGMP functions while γ is a continuous function. Suppose $g : S \to \mathbb{R}$ is a continuous set function. For all $\epsilon > 0$, there exists a function $f \in \mathcal{F}$, such that for any $S \in \mathcal{S}$,*

$$|g(S) - \gamma(f(S))| < \epsilon. \tag{10}$$

Proof of theorem 3. In this theorem we denote S as the representation of spatial network in Equation 1. Due to the continuity of g, we take δ_ϵ so that $|g(S) - g(S')| < \epsilon$ for any $S, S' \in \mathcal{S}$ if the Hausdorff distance between spatial information $d_H(S, S') < \delta_\epsilon$. Define the $\mathcal{K}_d, \mathcal{K}_\theta, \mathcal{K}_\varphi$ as the resolution of geometric features d, θ, φ, and without lossing generality, we can suppose $\mathcal{K} = \mathcal{K}_d = \mathcal{K}_\theta = \mathcal{K}_\varphi = \lceil \frac{1}{\delta_\epsilon} \rceil$. Let the mapping function Λ as $\Lambda(S) = \frac{\lfloor \mathcal{K}S \rfloor}{\mathcal{K}}$ which maps all the elements in an interval to the left end of the interval, such that we have $|g(S) - g(\Lambda(S))| < \epsilon$ for any $S \in \mathcal{S}$.

Let $f(S) \in \mathbb{R}^I$, where I is the number of dimension of embedding vectors for S. Then consider $f_\iota(S) = e^{||S - \hat{S}_\iota||_2}, \iota \in [1, ..., I]$, where $\hat{S}_\iota$ is one unit space in the transformed space of the mapping function Λ. Intuitively, we can consider each $f_\iota(S)$ measures if S is located in a unit $\hat{S}_\iota$ of the

18

discretized space by a smooth indicator. Similarly, we can define another mapping $\tilde{\xi}$ with discretize value as $\tilde{\xi}(S) = [\tilde{\xi}_1(S); \ldots; \tilde{\xi}_I(S)]$ with each $\tilde{\xi}_\iota(S) = 1$ indicating S is located in the ι-th unit, otherwise 0. The mapping from $f_\iota(S)$ to $\tilde{\xi}_\iota(S)$ can be easily learned by a linear function with ReLU as the activation function, which is exactly the setting in our framework. We denote this function as ω. We finally have $\tilde{\xi}(S) = \omega(f(S))$.

It is obvious that $\tilde{\xi}(S)$ is equivalent to $\Lambda(S)$. Let $\bar{\gamma}$ be a continuous function from $\mathbb{R}^I$ to $\mathbb{R}$ such that $\bar{\gamma}(\tilde{\xi}(S)) = g(\tilde{\xi}(S))$ and we can rewrite $\gamma = \bar{\gamma} \circ \omega$ Then

$$|\bar{\gamma}(\tilde{\xi}(S)) - g(S)|$$
$$= |\bar{\gamma}(\omega(f(S))) - g(S)|$$
$$= |\gamma(f(S)) - g(S)| < \epsilon$$

The proof is complete here. $\qquad\square$

Note: This proof is a generalization of the one by Qi *et al.* [71] on the point clouds data.

Proposition 1. *Let T denote a uniformly random spanning tree of a graph G. Then for a length three path $\pi_{ijkp} = (e_{ij}, e_{jk}, e_{kp})$ we have that*

$$\Pr(\pi_{ijkp} \in T) = det[Y_{\pi_{ijkp}}], \qquad (11)$$

where Y is called the *transfer function matrix* [9].
Proof of proposition 1. The number of spanning trees in a graph G is given by Kirchhoff's matrix tree theorem [14], showing that the number can be computed as $\mathrm{KMT}(G) = det\big[L[u]\big]$, where $L[u]$ is the graph Laplacian matrix L with its uth row and column removed, and u denotes a randomly chosen vertice. Obviously, the probability $\Pr(e_{ij} \in T)$ of sampling one edge e_{ij} in a random spanning tree T can be computed as

$$\Pr(e_{ij} \in T) = \frac{KMT(G) - KMT(\tilde{G}_{e_{ij}})}{KMT(G)},$$

where $\tilde{G}_{e_{ij}}$ is the graph G removed edge e_{ij}. Then we write

$$\Pr(\pi_{ijkp} \in T) = \Pr(e_{ij} \in T | e_{jk}, e_{kp} \in T)\Pr(e_{jk}, e_{kp} \in T)$$
$$= \Pr(e_{ij} \in T | e_{jk}, e_{kp} \in T)\Pr(e_{jk} | e_{kp} \in T)\Pr(e_{kp} \in T),$$

which can be formulated as

$$\Pr(\pi_{ijkp} \in T) = det[Y_{\pi_{ijkp}}],$$

given by Burton-Pemantle theorem [12]. We do not give the proof of Burton-Pemantle theorem here since it is not the focus of this paper. $\qquad\square$

Proposition 2. *If $\sigma^{(\ell)}$ is continuous, the expectation of the approximated form in Equation 7 converges surely to the original form in Equation 3 when the number of samples is sufficiently large.*
Proof of proposition 2. Because the random spanning trees are sampled i.i.d. from a uniform distribution, by the strong law of large number,

$$\tilde{h}_i^{(\ell+1)} = \mathrm{SUM}\big(\{\frac{m^{(\ell)}(\pi_{ijkp})}{q(\pi_{ijkp})} | \pi_{ijkp} \in \bar{\Pi}_{T,3}^i\}\big),$$

converges almost surely to the expected value $\mathrm{SUM}(m^{(\ell)}(\pi_{ijkp}))$. Then since $\sigma^{(\ell)}$ is continuous, by the continuous mapping theorem, the limits are preserved such that Equation 1

$$h_i^{(\ell+1)} = \sigma^{(\ell)}\Big(\mathrm{SUM}\big(\{\frac{m^{(\ell)}(\pi_{ijkp})}{q(\pi_{ijkp})} | \pi_{ijkp} \in \bar{\Pi}_{T,3}^i\}\big)\Big),$$

converges almost surely to Equation 3. $\qquad\square$

19

C Extra Experimental Settings

Implementation Details   The goal of the experiments is to validate the performance of our proposed model on spatial networks. We require all models follow the same architecture to utilize the same data for a fair comparison. Specifically, a single MLP layer m_1 is applied to the node attributes rather than the spatial information before the convolution layers. Then another MLP layer m_2 with decreasing hidden unit sizes is applied after the convolution layers. Each dataset excluding QM9 is split randomly 5 times into $80\% : 10\% : 10\%$ train, validation, and test. For the QM9 dataset we follow previous work's split [52]. For each split, we run each model 5 times to reduce the variance in particular data splits. Test results are according to the best validation results. For our accelerating method, we pre-sample and store the random spanning trees before the training phase. Note that even though we provide a novel Kirchhoff-normalized method to equivalent our sampled spanning trees to the original graph, the un-normalized version of our algorithm could also achieve competitive results in the experiments.

The following describes the details about our comparison models.

Graph Neural Networks (GNNs).

• *(i) GIN.* Graph Isomorphism Networks (GIN) [97] is a variant of GNN, which has provably powerful discriminating power among the class of 1-order GNNs;

• *(ii) GAT.* Graph Attention Networks (GAT) [83] uses multi-head attention layers to propagate information;

• *(iii) Gated GNN.* Gated Graph Sequence Neural Networks (Gated GNN) [58] use gated recurrent units (GRU) [19] as a recurrent function, reducing the recurrence to a fixed number of steps.

Spatial Neural Networks (SNNs).

• *(i) PointNet.* PointNet [71] learns pointwise features independently with several MLP layers and extracts global features with a max-pooling layer;

• *(ii) PPFNet.* Point Pair Feature Network (PPFNet) [26] is a spatial deep learning framework to learn a globally aware 3D descriptor;

• *(iii) SchNet.* SchNet [73] is a domain-specific model for predicting quantum chemistry. It utilizes a continuous filter function to the distances between nodes and their first-order neighbors.

• *(iv) DimeNet.* DimeNet [52] is another domain-specific model for predicting quantum chemistry, which includes the directional information by aggregating the *length two path* messages based on a physical representation of distances and angles.

Searching space for hyper parameters.
Number of epochs trained: $\{500\}$;
Size of each batch: $\{16, 64\}$;
Initial learning rate for model: $\{1e-3, 5e-3, 1e-4\}$;
Number of convolution layers: $\{1, 2, 3\}$;
Dimension of hidden state: $\{64\}$;
Weight decay ratio: $\{0.9\}$ (if error on validation set does not decrease for 10 epochs).

20